

## CROSS-SECTION MEASUREMENTS FOR RADIOACTIVE SAMPLES

Paul E. Koehler and Harold A. O'Brien

Los Alamos National Laboratory, Physics Division MS-D449  
Los Alamos, New Mexico 87545, USA

**Abstract:** The measurement of (n,p), (n, $\alpha$ ) and (n, $\gamma$ ) cross sections for radioactive nuclei is of interest to both nuclear physics and astrophysics. For example, using these reactions, properties of levels in nuclei at high excitation energies, which are difficult or impossible to study using other reactions, can be investigated. Also, reaction rates for both big-bang and stellar nucleosynthesis can be obtained from these measurements. In the past, the large background associated with the sample activity limited these types of measurements to radioisotopes with very long half-lives. The advent of the low-energy, high-intensity neutron source at the Los Alamos Neutron Scattering Center (LANSCE) has greatly increased the number of nuclei which can be studied. Examples of (n,p) measurements on samples with half lives as short as fifty-three days are given, and the nuclear physics and astrophysics to be learned from these data is discussed. Additional difficulties are encountered when making (n, $\gamma$ ) rather than (n,p) or (n, $\alpha$ ) measurements. However, with a properly-designed detector, and the high peak neutron intensities now available, (n, $\gamma$ ) measurements can be made for nuclei with half lives as short as several months. Progress on the Los Alamos (n, $\gamma$ ) cross-section measurement program for radioactive samples is discussed.

(Radioactive samples, neutron-induced cross sections, nuclear astrophysics, nuclear physics)

Introduction

There is much nuclear physics and nuclear astrophysics to be learned from the measurement of (n,p), (n, $\alpha$ ) and (n, $\gamma$ ) cross sections for radioactive nuclei. Due to the potentially large background associated with the sample activity, most measurements of this type have been limited in the past to stable nuclei or to isotopes with very long half lives. The advent of pulsed spallation neutron sources, such as one at the LANSCE<sup>1</sup>, have opened up the possibility of making cross-section measurements for neutron-induced reactions on nuclei with very short half lives. In this paper, some examples of recent measurements of this type are given and the physics that has been learned is discussed. Also, our plans for additional measurements are outlined together with the techniques involved and the expected results.

Experimental Techniques

The experimental technique used in our (n,p) and (n, $\alpha$ ) measurements<sup>2</sup>, and planned for the (n, $\gamma$ ) measurements<sup>3</sup>, has been published elsewhere so only the salient features will be presented here. Successful measurements require a large peak neutron intensity and a properly designed detector so that the observed rate for the reaction of interest is larger than the background rate associated with the decay of the sample under study. At the LANSCE<sup>1</sup>, the high peak neutron intensity is obtained by bombarding a tungsten target with an intense burst of protons. The protons are accelerated by the Los Alamos Meson Physics Facility (LAMPF) and compressed into an intense pulse by the newly commissioned Proton Storage Ring (PSR). At the design intensity of the PSR (100  $\mu$ A, at 12 Hz), the water moderated neutron intensity at 1 eV for a flight path of 7 m is  $4 \times 10^6$  neutrons/(eV cm<sup>2</sup> sec), and the neutron spectrum of this "white" source is approximately proportional to 1/E. The relatively long pulse width (270 ns) from the PSR limits the useful upper energy to about 50 keV at which point the energy resolution is about 25% for the 7 m flight path used in our measurements. The "white" nature of the neutron source means that measurements at all neutron energies are obtained simultaneously. This high neutron intensity allows measurements to be made with sample sizes in the 100 ng to few hundred  $\mu$ g range. Even these small samples can still present some rather

large background problems, but a properly designed detector can reduce the sample-related backgrounds to acceptable levels. Because the requirements for the detectors differ, the experimental techniques unique to the (n,p) and the (n, $\gamma$ ) measurements will be discussed separately below.

A\*(n,p) and A\*(n, $\alpha$ ) Measurements

For A\*(n,p) and A\*(n, $\alpha$ ) measurements, where A\* is a radioactive nucleus, the sample-related backgrounds can be reduced to manageable levels by choosing a charged-particle detector of thickness no greater than that needed to stop the protons or alphas from the reaction of interest. The detection efficiency for radioactive decay emissions from the sample can thus be reduced to the order of 10<sup>-6</sup> of the proton or alpha detection efficiency. Also, because very few nuclei emit charged particles under bombardment by slow neutrons, the sample can be of relatively low specific activity and can even be a chemical compound. The main requirements that the samples for these types of measurements must meet are: 1) The specific activity must be high enough that a sample which contains enough target nuclei is not too thick, and 2) the levels of contaminant <sup>6</sup>Li and <sup>10</sup>B, which have large (n, $\alpha$ ) cross sections, are low enough that they do not interfere with detecting the particles from the reaction of interest. For most (n,p) measurements, even these contaminants can be surmounted by the use of a  $\Delta$ E-E detector telescope.

To demonstrate the quality of the measurements possible, a typical subtracted spectrum from our <sup>22</sup>Na(n,p)<sup>22</sup>Ne and <sup>22</sup>Na(n, $\alpha$ )<sup>19</sup>F measurements is shown in fig. 1. These measurements were made with a sample containing approximately 75 ng of <sup>22</sup>Na ( $t_{1/2}$ =2.6 years). To our knowledge, these are the first measurements of the relatively small <sup>22</sup>Na(n, $\alpha$ )<sup>19</sup>F cross sections. Previous attempts to measure these cross sections were unsuccessful due to interference from a relatively large <sup>10</sup>B contamination in the sample<sup>4,5</sup> and/or due to the large background associated with the radioactive sample<sup>4,6</sup>. In our measurements, the <sup>10</sup>B contamination problem was overcome by the use of a very pure production target for the irradiation at the isotope production facility<sup>7</sup> at LAMPF, and very careful chemistry thereafter<sup>8</sup>. The background due to pileup from the radioactive decay products from the sample was overcome by the use of very thin detectors.

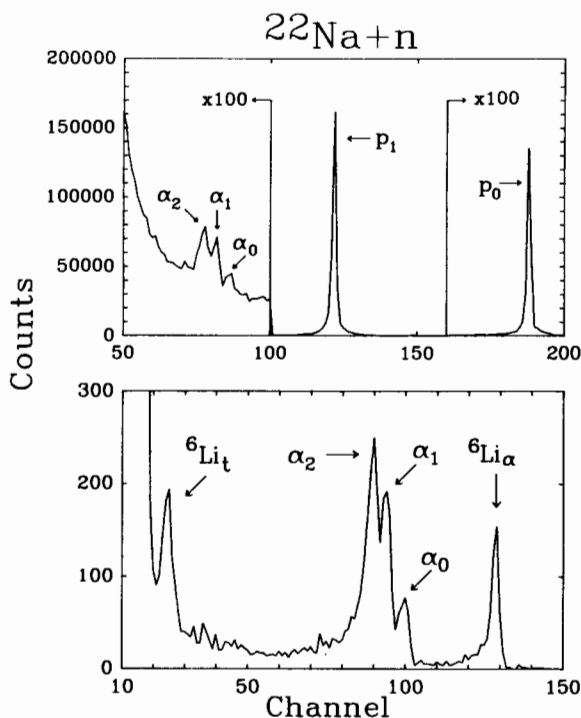


Fig. 1. Pulse-height spectra at thermal neutron energy from our  $^{22}\text{Na}+n$  measurements. The peaks are labeled according to the outgoing particle. These spectra were taken with a sample containing 75 ng of  $^{22}\text{Na}$ . The upper spectrum was taken with a detector which was 150  $\mu\text{m}$  thick by 25  $\text{mm}^2$  in area. The lower spectrum was taken with a detector of 10  $\mu\text{m}$  thickness by 50  $\text{mm}^2$  in area.

### $A^*(n,\gamma)$ Measurements

$A^*(n,\gamma)$  measurements require a separated isotopic sample on a low mass backing because many nuclei have sizable  $(n,\gamma)$  cross sections at low neutron energy. This requirement should not be too difficult to meet for the very small samples sizes required<sup>9-11</sup>. For these types of measurements the decay radiation from the sample is often of the same type as that from the reaction of interest. Pileup of these low-energy decay  $\gamma$ -rays can result in a signal the same size as that from a neutron-capture event. To overcome this potentially large background one can make use of the fact that the  $\gamma$ -ray decay energy,  $E_d$ , is almost always much less than the total energy,  $E_c$ , of the neutron capture cascade. Hence, a detector which registers all of the energy from the capture cascade, and which has a very short output pulse width,  $\tau$ , can effectively overcome this background. Of course, the size of this background is a very strong function of the ratio,  $E_d/E_c$ , and of  $\tau$ , and one can always think of very difficult cases for which measurements are still not possible. Our calculations show that measurements on many interesting samples with half lives as short as a several months can be made<sup>3</sup>.

A cube of barium fluoride ( $\text{BaF}_2$ ) covering almost  $4\pi$  in solid angle is an ideal choice for a capture detector for radioactive samples<sup>3</sup>. The high stopping power of  $\text{BaF}_2$  makes for a relatively compact (about 15 cm thick) detector, and the fast decay constant of its light output allows measurements on samples with short half lives. Finally, by lining the central beam hole with  $^{10}\text{B}_4\text{C}$ , the background from neutron scattering can be reduced to manageable levels for most samples of interest within the range of energies possible in our measurements.

In general, these measurements improve our understanding of nuclear physics by providing tests of nuclear models in a regime previously unexplored. This is most true for the  $A^*(n,\gamma)$  measurements where data can be obtained for a wide range of nuclei on both sides of the valley of beta stability. Specifically,  $(n,p)$  measurements provide information about the isospin mixing of the observed levels<sup>2</sup>,  $(n,\alpha)$  measurements provide tests of cluster models<sup>4</sup>, and, for all but the lightest nuclei studied, level density information can be obtained for levels of relatively high spin and high excitation.

Our  $^7\text{Be}(n,p)^7\text{Li}$  results<sup>2</sup> are one example of the interesting basic nuclear physics that is learned from these types of measurements. Our results, obtained using an approximately 90 ng sample of  $^7\text{Be}$  ( $t_{1/2}=53$  days), are shown in fig. 2. Also shown are the recent data of Gledenov *et al.*<sup>12</sup>. We did not observe the resonance suggested by Gledenov *et al.* at 170 eV.

Our R-matrix calculation<sup>2</sup> for this reaction, obtained from a fit to both our data as well as data from several other reactions proceeding through the  $^8\text{Be}$  compound nucleus is also shown in fig. 2. The cross section is dominated by a  $J^\pi=2^-$  resonance near threshold. Prior to our measurements and analysis, it was not totally understood why the width of the  $2^-$  resonance appeared to depend on the reaction used to observe it<sup>15</sup>. Also, the amount of isospin mixing in the resonance was variously reported to be either relatively large<sup>13,14,16</sup>, or very small<sup>15</sup>. Our new data and analysis<sup>2</sup> have resolved these apparent contradictions. The key to the solution is the fact that the pole in the S-matrix which describes this resonance is on an unphysical sheet remote from the physical sheet and, therefore, does not obey the usual unitary relations between its displacement from the real energy axis and the magnitude of its residue. As detailed in ref. 2, this location of the pole explains the reported observations<sup>13-15</sup> of widely different widths for this resonance as observed in different reactions. Also, because of the unusual position of this pole, it is necessary to be careful when evaluating the isospin mixing. Our analysis, which correctly takes into account the special position of this pole, leads to a higher T=1 isospin admixture (24%) for this predominantly T=0 resonance than that of other reported analyses<sup>15,16</sup>.

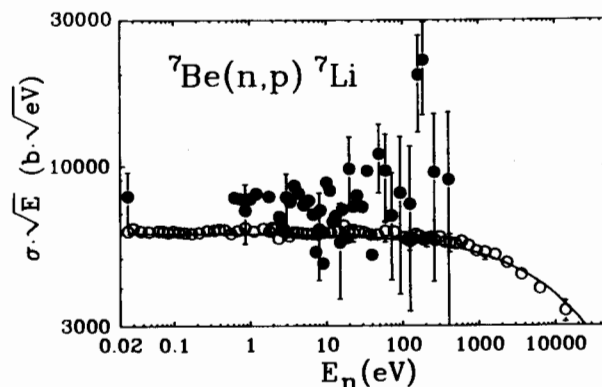


Fig. 2. The  $^7\text{Be}(n,p_0)^7\text{Li}$  reduced cross section versus laboratory neutron energy. Our data from ref. 2 are shown as open circles, while the data of ref. 12 are depicted as solid circles. For clarity, only every fifth data point of ours is shown below 100 eV. The solid curve is from an R-matrix fit to our data as well as data from other reactions as explained in ref. 2.

A second example of a longstanding puzzle is the nature of the structure of  $^{23}\text{Na}$  near the neutron threshold. Previous analyses of the measured  $^{22}\text{Na}(n,p)^{22}\text{Ne}$  cross sections<sup>4,5,6</sup> had assumed that a single level dominates both the  $p_0$  and  $p_1$  cross sections. Our measurements<sup>8</sup>, which were the first of the  $p_0$  cross section at other than thermal energy, have conclusively shown that at least two levels are needed to explain the data. As can be seen in fig. 3, the  $p_1$  cross section is dominated by a resonance at approximately 170 eV. In fig. 4, the measured  $p_0$  cross section is shown, along with the expected shape of the  $p_0$  cross section if the resonance seen in the  $p_1$  data was responsible for the  $p_0$  thermal cross section. Obviously, the  $p_1$  resonance contributes very little to the  $p_0$  cross section. Instead, the  $p_0$  cross section is dominated by another level in  $^{23}\text{Na}$ . It is most likely<sup>8</sup> that the  $p_0$  and  $p_1$  resonances have  $J^\pi=5/2^+$  and  $7/2^+$  respectively, and that the  $p_0$  resonance is probably the same as one observed in  $^{19}\text{F}(\alpha,p)^{22}\text{Ne}$  measurements<sup>17,18</sup>.

It is probably not unreasonable to expect that as we continue to make measurements more interesting information about specific levels will be learned, while overall the measurements will be helping to extend the general data base.

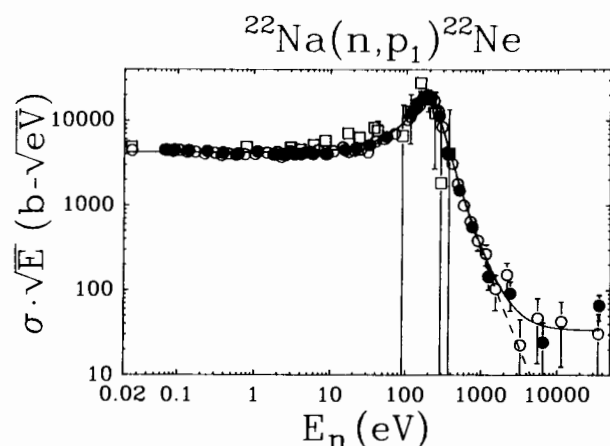


Fig. 3. The  $^{22}\text{Na}(n,p_1)^{22}\text{Ne}^*(1.27 \text{ MeV})$  reduced cross section versus laboratory neutron energy. Both the open and solid circles are our data from ref. 8. For clarity, only every fifth data point is shown below 100 eV. The squares are the data of ref. 6. The solid curve is a two-level, Breit-Wigner fit to our data, while the dashed curve is a single-level fit.

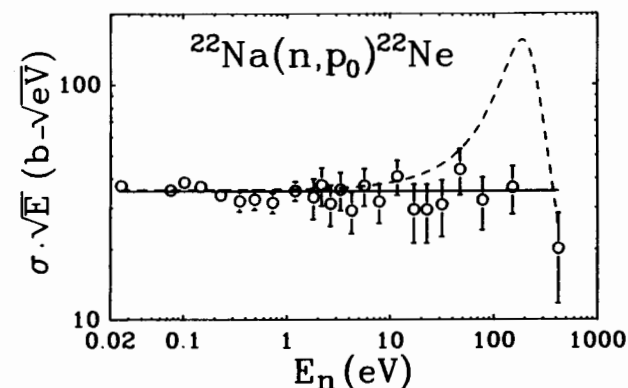


Fig. 4. The  $^{22}\text{Na}(n,p_0)^{22}\text{Ne}$  reduced cross section versus laboratory neutron energy. The open circles are our data from ref. 8. The dashed curve is the expected cross section if the resonance seen in the  $p_1$  data was responsible for the  $p_0$  thermal cross section, while the solid curve is from a fit to a strict  $1/v$  shape.

Over the years, cross sections for many reaction rates of importance to nucleosynthesis calculations have been measured in the laboratory. These rates have then been integrated into the reaction network used in the calculations and have improved the general understanding of several types of nucleosynthesis events. At present, the rates for several important reactions have not been measured, necessitating the use of theoretical estimates<sup>19</sup>. This may lead to large uncertainties in the isotopic yields from nucleosynthesis calculations. Many of the unmeasured rates involve neutron-induced reactions on radioactive nuclei<sup>20,21</sup>.

At Los Alamos, the very high peak intensity of the LANSCE white neutron source can be combined with laboratory facilities<sup>7</sup> for the production and separation of radioactive samples to open up new opportunities for nuclear astrophysics studies on unstable nuclei. For example, an active program to systematically measure the  $(n,\gamma)$  cross sections for radioactive branching points on the s-process nucleosynthesis path would help to finally reveal the physical conditions prevailing during stellar helium burning<sup>22</sup>. In addition, using these data to refine analyses will provide information on the dynamical aspects of the s-process, a problem where present stellar models fail to reproduce the observed isotopic abundances<sup>23</sup>. Also, measurements of  $(n,p)$  and  $(n,\alpha)$  cross sections for unstable nuclei will help reveal the conditions prevailing during explosive nucleosynthesis<sup>8</sup>, perhaps aiding in the explanation of the origin of radioisotopes observed by gamma-ray telescopes<sup>24,25</sup>, of the various isotopic anomalies observed in meteorites<sup>26</sup>, and of the production of several very rare stable isotopes<sup>20</sup>. Finally, measurements from this program will aid in the interpretation of several cosmochronometers, which will be useful in refining current estimates of the age of the universe. Below, we discuss the nuclear astrophysics that so far has been learned from our measurements, and indicate some of the things we hope to learn from future measurements.

A first example of an important  $A^+ + n$  reaction rate is  $^7\text{Be}(n,p)^7\text{Li}$ . This reaction is important to the nucleosynthesis of  $^7\text{Li}$  in standard hot big-bang calculations<sup>27-29</sup>. Prior to our measurements<sup>2</sup>, only the thermal cross section had been measured directly<sup>30</sup>. The rate<sup>31</sup> for this reaction used in calculations was based on the rather imprecise thermal measurement and on some  $^7\text{Li}(p,n)^7\text{Be}$  measurements<sup>13,14</sup> converted to  $(n,p)$  using detailed balance. Our data have substantially reduced (by a factor of almost ten at thermal energy) the uncertainty in the reaction rate. As can be seen in fig. 5, the rate based mainly on our results is only 60% to 80% of the old rate<sup>31</sup> in the temperature range of interest<sup>32</sup> (approximately 0.3 to 1 GK) in big-bang calculations. This difference can lead to as much as a 20% increase in the amount of  $^7\text{Li}$  calculated to be produced in the big bang<sup>2</sup>.

Our  $^{22}\text{Na}(n,p)^{22}\text{Ne}$  measurements<sup>8</sup> are a second example of a reaction involving a radioactive target which may be important in nucleosynthesis calculations. This reaction may play a role in the nucleosynthesis of  $^{22}\text{Na}$  and/or  $^{22}\text{Ne}$  in explosive environments. An understanding of the nucleosynthesis of these isotopes is important because the origin of the Neon-E anomaly in meteorites<sup>26</sup> is not well understood, and because  $^{22}\text{Na}$  has been suggested as a candidate for observation by gamma-ray telescopes<sup>33</sup>. The astrophysical reaction rate calculated from our data is compared to the theoretical rate<sup>19</sup> in fig. 6. At the energies where we can make measurements, most of the rate is due to protons emitted to the first excited state of  $^{22}\text{Ne}$ . The theoretical rate is about a factor of ten lower than the experimentally determined one at very low

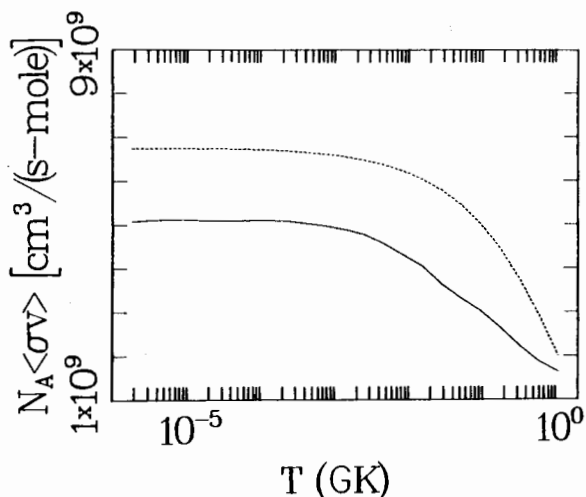


Fig. 5. The  ${}^7\text{Be}(n,p){}^7\text{Li}$  astrophysical reaction rate versus temperature. The solid curve is the rate calculated mainly from our data shown in fig. 2. The dashed curve is the theoretical estimate for this rate from ref. 31.

temperatures. However, due to the resonance at  $E_n=170$  eV, the two rates cross at 0.05 GK, and the theoretical rate is about a factor of six larger at the highest temperatures measured. If this difference between the experimental and theoretical rates persists to higher temperatures, it may result in a significant change in the calculated production of  ${}^{22}\text{Na}$  in explosive environments. For example, current estimates predict that approximately  $3 \times 10^{-5}$  solar masses of  ${}^{22}\text{Na}$  are produced in a 25-solar-mass supernova explosion<sup>34,35</sup>. From this it has been calculated that explosions of galactic supernovae probably would be observable with an orbiting gamma-ray telescope<sup>33,34</sup>. The reduction in the  ${}^{22}\text{Na}(n,p){}^{22}\text{Ne}$  reaction rate indicated by our measurements makes an observation even more probable should such an event occur. Calculations employing the new, lower rate which specifically address the production of  ${}^{22}\text{Na}$  are needed to understand quantitatively the effect of this change in the rate on the likelihood of observing  ${}^{22}\text{Na}$  with gamma-ray telescopes.

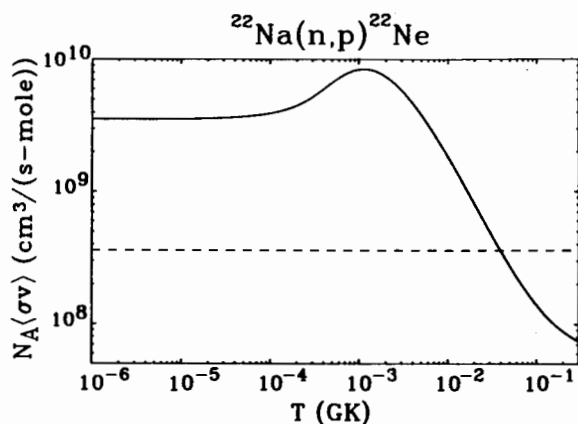


Fig. 6. The  ${}^{22}\text{Na}(n,p){}^{22}\text{Ne}$  astrophysical reaction rate versus temperature. The solid curve is the rate calculated from our data of ref. 8, while the dashed curve is the theoretical rate of ref. 19.

Our  ${}^{36}\text{Cl}(n,p){}^{36}\text{S}$  data will serve as a final example of how these measurements can contribute to nuclear astrophysics. These measurements were made with  $410 \mu\text{g}$  of  ${}^{36}\text{Cl}$ . Because the half life for this sample is long ( $t_{1/2}=3 \times 10^5$  years), a high peak neutron intensity is not essential to the measurements. However, the relatively high average neutron intensity available from the LANSCE is still important to measuring this comparatively small cross section within a reasonable time. Our preliminary data for energies greater than 700 eV are displayed in fig. 7. Because the thermal cross section has not yet been measured, we display yields rather than cross sections. The data reveal several resonances for energies greater than 800 eV. This reaction is denoted by an asterisk in Howard *et al.*<sup>20</sup>, a mark which they reserve for rates important to the nucleosynthesis of rare stable nuclei ( ${}^{36}\text{S}$  in this case) in explosive carbon burning. It remains to be seen how our measurements will affect the results of future nucleosynthesis calculations.

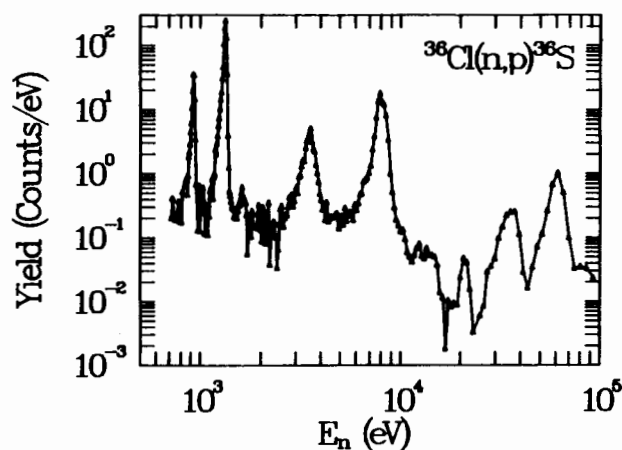


Fig. 7. Preliminary yield versus laboratory neutron energy from our  ${}^{36}\text{Cl}(n,p){}^{36}\text{S}$  measurements. The yield has not been corrected for the variation with energy of the neutron flux. Also, because we are currently measuring the absolute thermal cross section for this reaction, these yields have not yet been normalized to obtain cross sections.

#### Future Plans

Most of the measurements we have planned are motivated by the astrophysics to be learned, although the nuclear physics is also often very interesting. The largest potential impact of these measurements will probably come from the study of isotopic cross sections of interest to s-process and explosive nucleosynthesis calculations.

One example of cross sections of interest to both nuclear physics and astrophysics are those for the  ${}^{26}\text{Al}(n,p){}^{26}\text{Mg}$  reactions. From the nuclear physics standpoint, these measurements are interesting because they study states of high spin and high excitation in the compound nucleus  ${}^{27}\text{Al}$ . The information obtained from measuring the cross sections for these reactions could be important to theoretical level density calculations. The  ${}^{26}\text{Al}+n$  cross sections are also important for a better understanding of the environment in which explosive nucleosynthesis occurs. Although some measurements of this cross section have already been made<sup>36</sup>, the results are widely spaced in energy, and the reaction rate at low temperatures is not

well determined. Also, because most of the cross section is due to protons emitted to the first excited state of  $^{26}\text{Mg}$ , measurements made via the inverse reaction<sup>37,38</sup> determine only a small part of the total reaction rate. We are currently constructing a target station to be installed in a low-energy accelerator. With this apparatus we will make an  $^{26}\text{Al}$  sample for measurements at the LANSCE. This should allow us to measure the  $^{26}\text{Al}(n,p)^{26}\text{Mg}$  cross sections from thermal energy to approximately 50 keV.

Other nuclei for which  $A^*(n,p)$  and  $A^*(n,\alpha)$  measurements are possible at the LANSCE and which are of interest to nuclear astrophysics<sup>20</sup> include  $^{37}\text{Ar}$  and  $^{41}\text{Ca}$ . We hope to measure the cross sections for these nuclei in the future. We have already made preliminary (n,p) measurements for the stable nuclei  $^{14}\text{N}$  and  $^{35}\text{Cl}$ , and plan to extend these measurements in the near future.

Potentially, the largest number of measurements to be made are of  $A^*(n,\gamma)$  cross sections which are mainly of interest for a better understanding of s-process nucleosynthesis. Once our  $A^*(n,\gamma)$  detector is operational, we will begin these measurements with an isotope such as  $^{170}\text{Tm}$  ( $t_{1/2}=128.6$  days) which has been predicted by theory to have the largest cross section in a region of branching in the s-process flow. Such isotopes determine the "freeze-out" time<sup>22</sup>, an important parameter used in the comparison of the neutron density determined from empirical or "classical" calculations to the density calculated by stellar models. The first couple of measurements of this type will help to put more stringent limits on the mean properties of the s-process environment. After more measurements, the inconsistencies in the mean properties obtained from the "classical" analyses of the different branching points will lead to a better understanding of the dynamics of the s-process environment<sup>22</sup>. These measurements on radioactive samples, coupled with the planned very precise measurements on stable isotopes<sup>39</sup>, and new calculational approaches<sup>23</sup> should lead to a much better understanding of the s-process, including its dynamics.

#### Acknowledgements

The authors are indebted to several people who have been instrumental to the continuing success of the program of measurements presented here. We would like to thank C.D. Bowman for his considerable help in getting this program underway and the first measurements on  $^7\text{Be}$  completed, and for many helpful discussions. We would also like to thank P.W. Lisowski, E.D. Arthur and D.W. Barr for their support of this program. These measurements were supported by the U.S. Department of Energy.

#### REFERENCES

- 1) R.N. Silver, *Physica* **137B**, 359 (1986).
- 2) P.E. Koehler *et al.*, *Phys. Rev. C* **37**, 917 (1988).
- 3) P.E. Koehler, H.A. O'Brien and C.D. Bowman, to be published in the *Proceedings of the Workshop on Nuclear Spectroscopy of Astrophysical Sources* (Washington, D.C., 1988).
- 4) J. Kvitek, V. Hnatowicz, J. Cervena, J. Vacik and V.M. Gledenov, *Z. Phys.* **A299**, 187 (1981).
- 5) R. Ehehalt, H. Morinaga and Y. Shida, *Z. Naturforsch* **26a**, 590 (1971).
- 6) Yu. M. Gledenov *et al.*, *Z. Phys.* **A308**, 57 (1982).
- 7) H.A. O'Brien, Jr., A.E. Ogard and P.M. Grant, *Prog. Nucl. Med.* **4**, 16 (1978).
- 8) P.E. Koehler and H.A. O'Brien, Submitted for publication to *Phys. Rev. C*.
- 9) R.A. Naumann *et al.*, *Nucl. Instr. Meth.* **B26**, 59 (1987).

- 10) S.B. Karmohapatro, *Nucl. Instr. Meth.* **B26**, 34 (1987).
- 11) E. Hechtel, *Nucl. Instr. Meth.* **B26**, 37 (1987).
- 12) Yu. M. Gledenov *et al.*, *JINR Rapid Communications*, **17-86**, 36 (1986).
- 13) H.W. Newson, R.M. Williamson, K.W. Jones, J.H. Gibbons and H. Marshak, *Phys. Rev.* **108**, 1294 (1957).
- 14) R.L. Macklin and J.H. Gibbons, *Phys. Rev.* **109**, 105 (1958); J.H. Gibbons and R.L. Macklin, *Phys. Rev.* **114**, 571 (1959).
- 15) L.G. Arnold, R.G. Seyler, L. Brown, T.I. Bonner and E. Steiner, *Phys. Rev. Lett.* **32**, 895 (1974); L. Brown, E. Steiner, L.G. Arnold and R.G. Seyler, *Nucl. Phys.* **A206**, 353 (1973).
- 16) F.C. Barker, *Aust. J. Phys.* **30**, 113 (1977).
- 17) R. Ehehalt, Y. Shida, C. Signorini and H. Morinaga, *Nuovo Cimento*, **15A**, 209 (1973).
- 18) J. Kuperus, *Physica* **31**, 1603 (1965).
- 19) See for example, S.E. Woosley *et al.*, *At. Data Nucl. Data Tables* **22**, 371 (1978).
- 20) W.M. Howard *et al.*, *Ap. J.* **175**, 201 (1972).
- 21) G.J. Mathews *et al.*, in *Nuclear Data for Basic and Applied Science, Vol. I*, P.G. Young, R.E. Brown, G.F. Auchampauch, P.W. Lisowski and L. Stewart, eds. (Gordon and Breach, New York 1986) p 835, 927.
- 22) F. Kappeler *et al.*, *Ap. J.* **257**, 821 (1982).
- 23) W.M. Howard *et al.*, *Ap. J.* **309**, 633 (1986).
- 24) W.A. Mahoney, J.C. Ling and A.S. Jacobson, *Ap. J.* **262**, 742 (1982).
- 25) S.M. Matz *et al.*, to be published in the *Proceedings of the Workshop on Nuclear Spectroscopy of Astrophysical Sources*, (Washington, D.C., 1988)
- 26) See for example, D.C. Black, *Geochim. Cosmochim. Acta.*, **36**, 377 (1972).
- 27) G. Beadet and H. Reeves, *Astron. Astrophys.* **134**, 240 (1984).
- 28) J. Yang *et al.*, *Ap. J.* **281**, 493 (1984).
- 29) P. Delbourgo-Salvador, C. Gry, G. Malinie and J. Audouze, *Astron. Astrophys.* **150**, 53 (1985).
- 30) R.C. Hanna, *Phil. Mag.* **46**, 381 (1955).
- 31) N.E. Bahcall and W.A. Fowler, *Ap. J.* **157**, 659 (1969).
- 32) A.M. Boesgaard and G. Steigman, *Ann. Rev. Astron. Astrophys.* **23**, 319 (1985).
- 33) See for example, D.D. Clayton, *Ap. J.* **198**, 151 (1975).
- 34) S.E. Woosley and T.A. Weaver, *Ap. J.* **238**, 1017 (1980).
- 35) S.E. Woosley and T.A. Weaver, in *Essays in Nuclear Astrophysics*, C.A. Barnes, D.D. Clayton and D.N. Schramm, eds. (Cambridge Univ. Press, 1982) p. 377.
- 36) H.P. Trautvetter *et al.*, *Z. Phys.* **A323**, 1 (1986).
- 37) R.T. Skelton, R.W. Kavanagh and D.G. Sargood, *Phys. Rev. C* **35**, 45 (1987).
- 38) G. Doukellis and J. Rapaport, *Nucl. Phys.* **A467**, 511 (1987).
- 39) K. Wisshak, K. Guber and F. Kappeler, *Nucl. Instr. Meth.* **A259**, 583 (1987) and references contained therein.